Acta Oceanol. Sin., 2025, Vol. 44, No. 4, P. 90–100
https://doi.org/10.1007/s13131-024-2445-1

Distribution patterns of nitrous oxide during the summer season in the Prydz Bay, eastern Southern Ocean

Jiexia Zhang[1], Damian L. Arévalo-Martínez[2, 3, 4, 5], Liyang Zhan[1*], Liqi Chen[1], Jun Zhao[6], Wangwang Ye[1], Man Wu[1], Yuhong Li[1], Jian Liu[1]

[1] Key Laboratory of Global Change and Marine Atmospheric Chemistry, Third Institute of Oceanography, Ministry of Natural Resources, Xiamen 361005, China

[2] RD2 Marine Biogeochemistry, GEOMAR Helmholtz Centre for Ocean Research Kiel, Kiel 24148, Germany

[3] Institute of Geosciences, Kiel University, Kiel 24148, Germany

[4] Microbiology Department, Radboud University Nijmegen, Nijmegen 6525XZ, The Netherlands

[5] Leibniz Institute for Baltic Sea Research Warnemünde, Rostock 18119, Germany

[6] Key Laboratory of Marine Ecosystem Dynamics, Second Institute of Oceanography, Ministry of Natural Resources, Hangzhou 310012, China

Received 14 October 2024; accepted 21 January 2025

© Chinese Society for Oceanography and Springer-Verlag GmbH Germany, part of Springer Nature 2025

Abstract

The global ocean is a major source of the climate-relevant atmospheric trace gas nitrous oxide (N_2O). However, an accurate assessment of the global oceanic emissions of N_2O is hampered by missing data on dissolved N_2O from large regions such as the Southern Ocean. To address this deficit, N_2O was measured in the Prydz Bay in February 2015 during the 31st Chinese National Antarctic Research Expedition. N_2O concentrations (saturation) in the surface layer were generally low (undersaturation with respect to atmospheric equilibrium) and ranged from 13.3 nmol/L to 16.1 nmol/L (83%–102%) at the time of sampling. A comparison of our observations with archived data revealed that no discernible trend in N_2O concentrations in the surface waters of Prydz Bay could be detected for the period between 2006 and 2015. Temperature and salinity changes driven by meltwater input were the predominant controls on N_2O concentrations in surface waters. At depth, the distribution of N_2O concentrations was dominated by production via nitrification in offshore deep waters and vertical convection in the shelf waters, where concentrations were lower and gradients were less steep. Our results suggest a rather unusual pattern of N_2O distribution in the Prydz Bay (low N_2O in shelf waters compared with the open ocean), providing important insights into the coastal dynamics of N_2O in high-latitude polar regions.

Key words nitrous oxide (N_2O), greenhouse gases, sea-to-air flux, Prydz Bay, Southern Ocean

Citation Zhang Jiexia, Arévalo-Martínez Damian L., Zhan Liyang, Chen Liqi, Zhao Jun, Ye Wangwang, Wu Man, Li Yuhong, Liu Jian. 2025. Distribution patterns of nitrous oxide during the summer season in the Prydz Bay, eastern Southern Ocean. Acta Oceanologica Sinica, 44(4): 90–100, doi: 10.1007/s13131-024-2445-1

1 Introduction

Nitrous oxide (N_2O) is an important atmospheric greenhouse gas because of its strong radiative effect, which is 200−300 times greater than that of carbon dioxide (Canadell et al., 2021), and its role as a major ozone-depleting substance in the stratosphere (Ravishankara et al., 2009). Since the Industrial Revolution, the volume fraction of N_2O concentration in the atmosphere has increased by about 24%, from 270 ppbv in 1750 to about 336 ppbv in 2023 (Dutton and Hall, 2023).

Marine production mainly occurs via two microbial pathways, namely, nitrification and denitrification. Under oxic conditions, N_2O results as a byproduct of the first

Foundation item: The National Natural Science Foundation of China under contract No. 41906193; the Scientific Research Foundation of Third Institute of Oceanography, Ministry of Natural Resources, under contract No. 2019033; the Natural Science Foundation of Fujian Province under contract No. 2019J05147; the Federal Ministry of Education and Research of Germany under contract No. FKZ 03F03F0783A; the National Polar Special Program under contract Nos IRASCC 01-01-02 and IRASCC 02-02.

*Corresponding author, E-mail: zhanliyang@tio.org.cn

step of bacterial and archaeal nitrification (i.e., the oxidation of ammonia to nitrite), and the N_2O yield during nitrification increases with decreasing oxygen concentration (Goreau et al., 1980; Löscher et al., 2012). During denitrification, N_2O results as an intermediate product through nitrite reduction under suboxic conditions. Under oxygen concentrations below approximately 5 μmol/L, N_2O is reduced to nitrogen gas during complete denitrification (Zhang et al., 2020).

Oceans are generally considered a net source of atmospheric N_2O. Based on *in situ* observations and model estimates, surface ocean waters constitute 3.4 Tg/a (2.5–4.3 Tg/a), in terms of N, of the total N_2O source (about 17.0 Tg/a, in terms of N) (Tian et al., 2020). The eastern tropical Pacific, equatorial and coastal upwelling zones are thought to be the largest oceanic N_2O emission regions (Yang et al., 2020), whereas open ocean waters are mostly near atmospheric equilibrium. High-latitude (polar) studies are scarce, and consequently, uncertainties regarding N_2O source-sink dynamics and marine emissions from the open ocean (Yang et al., 2020) and coastal areas (Resplandy et al., 2024) remain largely uncertain.

The Southern Ocean (SO) occupies about 20% of the global ocean area, yet the extent of N_2O exchange across sea-ice-air interfaces is poorly understood. To date, only a few studies have published results on N_2O measurements from the SO (Rees et al., 1997; Farías et al., 2015; Zhan et al., 2015; Grefe et al., 2018). Based on the evaluation of high-resolution air N_2O measurements at the atmospheric monitoring station Cape Grim, Tasmania (Australia), Nevison et al. (2005) estimated that approximately 0.9 Tg/a, in terms of N, is ventilated to the atmosphere as N_2O in the SO (30°–90°S). Hence, the SO may account for approximately 21% of global oceanic N_2O emissions (Tian et al., 2020), which suggests that the region might be a potential source for the atmosphere. However, the region estimated based on the extrapolation of the dataset (Weiss et al., 1992) covered latitudes between 40°S and 60°S, and field studies have shown slight undersaturation of N_2O (90%–94%) in the Antarctic coastal zone (Rees et al., 1997; Zhan et al., 2015), indicating that the SO could also act as a N_2O sink. The Antarctic coastal zone is covered by sea ice all year round except in summer. As shown by recent studies, sea ice can act as a reservoir of organic matter (Henley et al., 2023; Koch et al., 2023; Thomas et al., 2001), which might fuel N_2O production during organic matter degradation. The produced N_2O could then be released into the atmosphere at the beginning of sea ice melting. In addition, sea ice-influenced coastal waters might become sinks (Rees et al., 1997; Zhan et al., 2015) due to the dilution of meltwater (Rees et al., 2022). In recent decades, global climate change has caused rapid changes in the SO, including warming (Sallee, 2018), westerly wind strengthening (Thomson et al., 2002) and altered temporal variability in sea ice formation-melting cycles (Kurtz and Markus, 2012). Ocean warming might change the activity of bacteria or archaea and hence change the N_2O production rate. The increase in ocean temperature also accelerates the melting of sea ice, which could promote productivity by facilitating iron inputs from the Antarctic ice sheet (St-Laurent et al., 2017) and increasing sunlight exposure (Castellani et al., 2022), potentially affecting surface productivity, which, upon sinking, would fuel N_2O production. However, unlike in the open ocean, the presence of melting sea ice in the Antarctic coastal zone enhances stratification, which could result in a dilution effect that reduces surface N_2O concentrations while increasing storage at greater depths (Randall et al., 2012; Zhan et al., 2015). At present, it is unclear how the interactions between these processes affect the SO N_2O budget.

To determine whether these ongoing changes affect N_2O distributions and sea-air emissions and how they affect the eastern SO, we conducted a multiyear survey of N_2O in the Prydz Bay (the third largest embayment in Antarctica). Here, we present measurements of dissolved N_2O from this area in February/March 2015. These measurements were complemented with archived records of N_2O measurements from January 2006 (Zhan and Chen, 2009) and 2011 (Zhan et al., 2015) to decipher the variability in dissolved N_2O in the Prydz Bay under a changing SO. The possible influencing factors were discussed in combination with the environmental parameters. Our findings offer new insights into N_2O dynamics in high-latitude marine environments.

2 Material and methods

2.1 *Study site*

Seawater samples for the determination of N_2O concentrations were collected from four sections (P5, P6, PA, and IS) in the Prydz Bay (64°00′–70°00′S, 72°00′–76°00′E; 3−10 February 2015) as part of the 31st Chinese National Antarctic Research Expedition (CHINARE) aboard the research vessel *Xuelong* (Fig. 1a). The transect extended from the front of the Amery Ice Shelf to the continental shelf (with depth < 1 000 m) and to the offshore deep waters (Fig. 1a). The data from the 31st CHINARE were complemented by the data from the 22nd and 27th CHINARE cruises (Fig. 1b), which took place in January 2006 (Zhan and Chen, 2009) and January 2011 (Zhan et al., 2015) (Table 1). Notably, only surface measurements are available for the 22nd CHINARE.

2.2 *Analysis and data handling*

2.2.1 *N_2O concentrations*

Water samples were collected from Niskin bottles that were mounted on a Conductivity-Temperature-Depth (CTD) rosette. Seawater was transferred from the Niskin bottles to 250 mL BOD bottles via a silicon tube. After overflowing 2–3 times the bottle volume, 0.1 mL of satu-

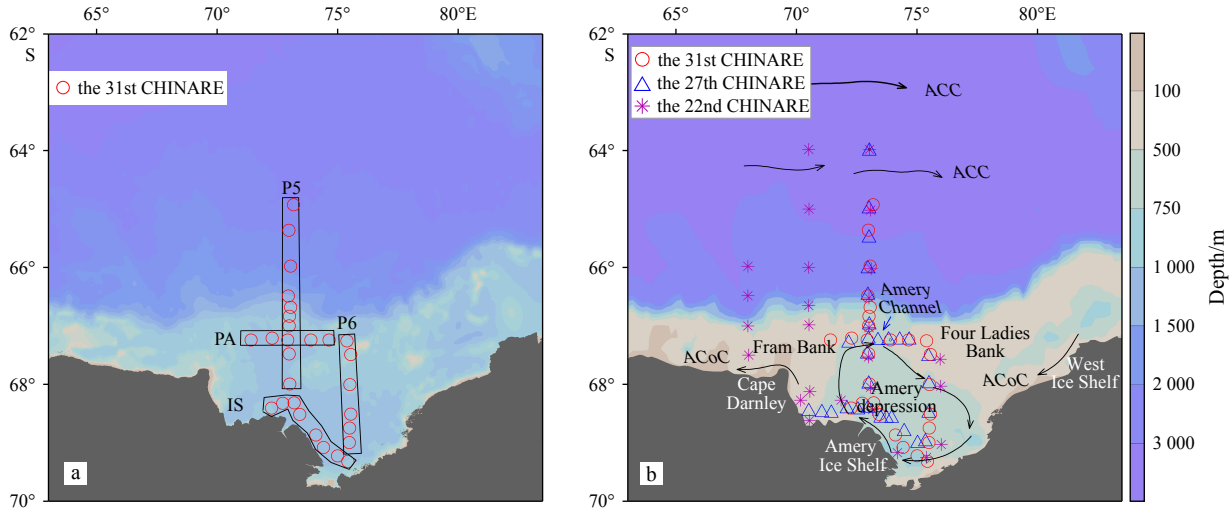


Fig. 1. Study location and distribution of sampling sites in the Prydz Bay. a. Four transect (P5, P6, PA, and IS) samples that taken during the 31st CHINARE, and b. sampling sites during the 31st CHINARE (red cycle), 27th CHINARE (blue triangle) and 22nd CHINARE (purple asterisk). A relatively narrow and cold coastal current (Antarctic Coastal Current, ACoC) from the West Ice Shelf penetrates into the southeastern part of the bay. North of the continental shelf, the main flow is associated with the Antarctic Circumpolar Current (ACC).

Table 1. Dissolved surface N_2O concentrations and saturation during the 22nd, 27th, and 31st CHINARE periods in the Prydz Bay

Cruise	Sampling date	Atm. N_2O volumn fraction/ppbv	SST/℃	Salinity	N_2O concentration/ (nmol·L^{-1})	N_2O average (range) saturation/%
22nd CHINARE	14–24 Jan. 2006	318.30	–1.1–3.5	29.8–34.6	12.5–15.3	99 (84–114)
27th CHINARE	4–5 Jan. 2011	323.23	–1.7–2.0	33.0–34.1	13.6–16.8	94 (88–102)
31st CHINARE	3–10 Feb. 2015	326.81	–1.6–0.9	32.0–33.4	13.3–16.1	94 (83–102)

Note: The data from the 22nd and 27th CHINARE cruises are from Zhan and Chen (2009) and Zhan et al. (2015), respectively. Please note that the N_2O concentrations from the 31st CHINARE have been corrected (see above). Atmospheric (Atm.) N_2O dry mole fractions were measured at Syowa Station (Antarctica) (Dutton and Hall, 2023).

rated mercuric chloride ($HgCl_2$) was added to the bottles to inhibit microbial activity. The bottles were immediately sealed with greased ground-glass stoppers and fastened with a clip to avoid air contamination. All the seawater samples had no bubbles and were stored at 4℃. In the laboratory, bubble-free, triplicate subsamples were taken from 250 mL BOD bottles into 20 mL headspace vials and then crimped with a metal crimp cap with PTFE-coated silicone rubber septa. Approximately 10 mL of high-purity nitrogen (N_2, 99.999%) was used to create a headspace by replacing the seawater with N_2. The N_2O contents of the samples were analyzed via a static headspace method coupled with gas chromatography (GC-2010, SHIMADZU, Japan) equipped with an electron capture detector (ECD) (Zhan et al., 2013). Aqueous standard solutions were made of N_2O standard gas-equilibrated water, and a headspace was created by following the same protocol as for the seawater samples. Six standard gas mixtures (volume fraction 100 ppbv, 200 ppbv, 300 ppbv, 500 ppbv, 700 ppbv, and 900 ppbv N_2O in N_2) were used. The standard gas mixtures were purchased from the National Institute of Metrology (NIM), P. R. China, and were calibrated against standard gas mixtures from the NOAA Earth System Research Laboratory. The NIM standards were within ±0.5% (or better) of the NOAA reference standards. The overall mean relative precision of the dissolved N_2O concentrations was ±2%. The calculation of the N_2O concentrations is described by Zhan et al. (2013).

2.2.2 *N_2O saturation and excess*

The saturation (in %) and excess N_2O concentration (ΔN_2O) were calculated via the following equations:

$$N_2O_{saturation} = [N_2O]_{measured}/[N_2O]_{eq} \times 100\%, \quad (1)$$

$$\Delta[N_2O] = [N_2O]_{measured} - [N_2O]_{eq}, \quad (2)$$

where $[N_2O]_{eq}$ is the equilibrium concentration of N_2O at the *in situ* seawater temperature and salinity at the time of sampling, computed with the solubility equation by Weiss and Price (1980) and using a mean monthly atmospheric N_2O dry mole fraction of 326.81 nmol/mol measured at mole fraction the Syowa Station (Antarctica; https://www.esrl.noaa.gov/gmd/hats/combined/N_2O.html).

2.2.3 *Data comparability*

We calibrated N_2O concentrations during different cruises by comparing the values in deep waters. We assumed that the N_2O concentrations in deep waters (>3 000 m) of Prydz Bay were stable within the relatively short period considered here (Bange and Andreae, 1999; Toyoda et al., 2019). The N_2O concentrations in deep ocean waters were compared to correct the measurement error between different cruises. As a result, we found that the N_2O concentrations in deep waters were slightly higher during the 31st CHINARE than during the 27th CHINARE. Consequently, a correction factor of 0.93 was applied. The correction factor resulted from the ratio of the mean N_2O concentrations in deep waters between the 27th CHINARE and 31st CHINARE. All N_2O concentrations from the 31st CHINARE were multiplied by this factor. The N_2O concentration data from the 22nd CHINARE were not corrected because only surface water data were available. The analytical precision of this dataset was ±5%.

2.2.4 *Other parameters*

Nutrients and dissolved oxygen (O_2) were obtained from the Second Institute of Oceanography, Ministry of Natural Resources. The nutrients were measured via Ultraviolet-Visible spectrophotometry, with a precision of ±0.1 μmol/L for NO_3^- according to the WOCE protocol (Sun et al., 2012). The O_2 concentrations were determined via the automatic Winkler titration method, with a precision of ±1 μmol/L. Apparent oxygen utilization (AOU) was calculated via the following equation:

$$\mathrm{AOU} = [\mathrm{O_2}]_{\mathrm{eq}} - [\mathrm{O_2}]_{\mathrm{meas}}, \tag{3}$$

where $[O_2]_{eq}$ is the equilibrium concentration calculated with the *in situ* seawater temperature and salinity via the O_2 solubility equation from Weiss (1970) and where $[O_2]_{meas}$ is the measured *in situ* O_2 concentration.

The temperature and salinity data were obtained from a calibrated SBE-911 conductivity-temperature-depth (CTD) system (Sea-Bird Electronics Inc., America). The CTD temperature and salinity precision were 0.001℃ and 0.002, respectively.

2.2.5 *Sea-air flux*

Sea-to-air flux densities ($F_{\mathrm{sea\text{-}air}}$ in μmol/(m²·d) of N_2O) were computed via surface layer (3–5 m depth) data by applying Eq. (4):

$$F_{\mathrm{sea\text{-}air}} = k \times \Delta[\mathrm{N_2O}], \tag{4}$$

where the gas transfer velocity (k, in cm/h) was computed according to Wanninkhof (2014):

$$k_w = 0.251(u_{10})^2(Sc_{\mathrm{N_2O}}/660)^{-0.5}, \tag{5}$$

where u_{10} represents the wind speed at a height of 10 m above sea level, which was obtained from the ship's anemometer. Sc_{N_2O} is the Schmidt number for N_2O computed via the empirical equation from Wanninkhof (2014):

$$Sc_{\mathrm{N_2O}} = 2\,356.2 - 166.38\,t + 6.395\,2\,t^2 - 0.134\,22\,t^3 + 0.001\,150\,6\,t^4, \tag{6}$$

where t is the temperature of seawater.

2.2.6 *N_2O mass balance calculation in the surface mixed layer*

The depth of the surface mixed layer (SML) was defined based on a potential density difference of 0.125 kg/m³ and a temperature difference of 0.5℃ within the surface water (<2 m) (de Boyer Montégut et al., 2004; Ye et al., 2023). N_2O fluxes through the pycnocline into the SML due to turbulent diffusivity (F_{deep}) were estimated as follows:

$$F_{\mathrm{deep}} = K_z \frac{\partial [\mathrm{N_2O}]}{\partial z}, \tag{7}$$

where K_z represents the diffusion coefficient at depth z (in m) and 10^{-4} m²/s was used as the value in the Southern Ocean (Mashayek et al., 2017). $\frac{\partial [\mathrm{N_2O}]}{\partial z}$ is the vertical N_2O gradient. Considering that the surface water in the Prydz Bay is a closed cyclonic and weak gyre, the effect of upwelling due to Ekman offshore water transport was assumed to be of minor importance (Charpentier et al., 2010). We used a simple mass balance approach between the upward N_2O fluxes through the pycnocline and the outward fluxes through the sea-air interface (Fig. 2). The balance is expressed as follows:

$$-F_{\mathrm{sea\text{-}air}} + F_{\mathrm{deep}} + P_i + F_x = 0, \tag{8}$$

where P_i [μmol/(m²·d)] represents the integrated N_2O production in the SML (Charpentier et al., 2010). F_x is the other N_2O source/sink generated by physical processes such as meltwater intruding the SML. A positive value of F_x corresponds to the input of N_2O from meltwater, a negative value of $F_{\mathrm{sea\text{-}air}}$ corresponds to ocean uptake of atmospheric N_2O, and a positive value of F_{deep} corresponds to the input of N_2O from the subsurface to the SML.

3 Results

3.1 *Oceanographic setting*

Prydz Bay is the third largest bay of the SO and has a unique topographic setting. The shelf oceanic circulation is characterized by a closed cyclonic gyre centered in a

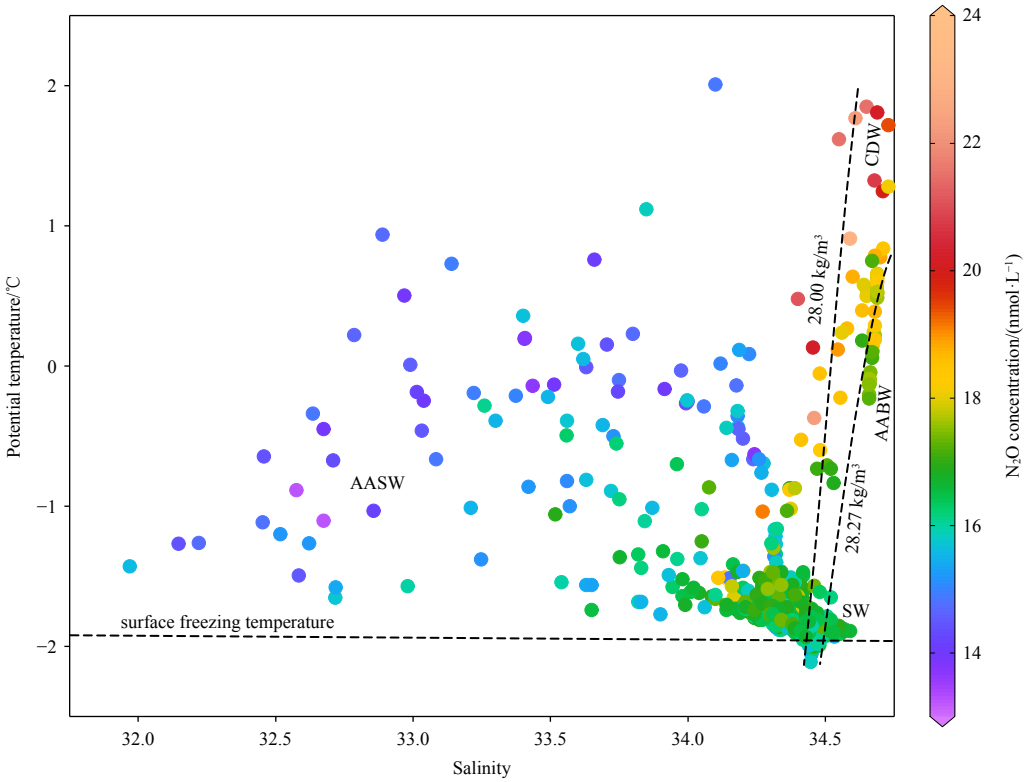


Fig. 2. Potential temperature-salinity scatter plot for the sampling stations from the 27th CHINARE and 31st CHINARE, colored for N_2O concentration at all stations. The two neutral density dashed lines represent the 28.00 kg/m^3 and 28.27 kg/m^3 surfaces, which are used to define Antarctic Summer Surface Water (AASW) and to separate Circumpolar Deep Water (CDW) from Antarctic Bottom Water (AABW). The dashed horizontal line shows the surface freezing temperature of the seawater. SW: continental shelf water.

deep channel, known as the Amery Depression (Smith et al., 1984; Vaz and Lennon, 1996) (Fig. 1b). A relatively narrow and cold coastal current (Antarctic Coastal Current, ACoC) runs from the West Ice Shelf and enters the southeastern part of the bay. When the ACoC reaches the shallow region and near the Amery Ice Shelf, two components affect the flow, resulting in the formation of the typical gyre circulation in the area: one component of the current toward the west and the other eastward back to the inner region of the shelf (Smith et al., 1984; Sabu et al., 2021). The flow north of the continental shelf is associated with the Antarctic Circumpolar Current (ACC), which is driven eastward by the prevailing westerlies (Fig. 1b; Smith et al., 1984).

The continental shelf and offshore deep-water regions in the Prydz Bay are separated by a frontal structure, the Antarctic slope front (ASF), which extends from the shelf break (about 66.8°S) and ascends northward to subsurface layers (Williams et al., 2010). The major water masses identified in the Prydz Bay during austral summer are Antarctic surface water (AASW), continental shelf water (SW), Circumpolar Deep Water (CDW), and Antarctic Bottom Water (AABW). AASW has variable characteristics in terms of temperature and salinity ($T > -1.80$℃, $S < 34.45$) (Wong et al., 1985), with a neutral density (γ_n) < 28.00 kg/m^3 (Shadwick et al., 2014), and is located in the upper layer from about 20 m within the Prydz Bay to approximately 80 m in the oceanic domain (Wong et al., 1985). Below the AASW lies a temperature minimum layer (-1.9℃ < T < -1.5℃, 34.2 < S < 34.5) (Wong et al., 1985), which is a layer of remnant "memory" of surface water formed in winter and called winter water (WW). To distinguish the WW in the continental shelf and offshore oceanic domain separated by the ASF (Smith et al., 1984; Middleton and Humphries, 1989), the continental shelf water, which is called SW, occupies most of the water column due to deep overturning derived from cool air temperature, strong winds and salt rejection during the formation of sea ice in winter. In the oceanic domain, it is termed WW and reaches a depth that gradually decreases northward from 300 m at about 67°S to disappear at about 64°S (Anilkumar et al., 2006). Below WW is CDW, which is warm, saline (0℃ < T < 2℃, 34.67 < S < 34.75) (Wong et al., 1985), and depleted of oxygen with a density of 28.00 kg/m^3 < γ_n < 28.27 kg/m^3 (Shadwick et al., 2014). The southward flowing warming CDW mixes with ambient water masses in the shelf region and forms modified Circumpolar Deep Water (mCDW) (Lin et al., 2016). Below the CDW is the AABW, which has a temperature of about 0℃ and a salinity of about 34.67 (Fig. 2).

3.2 N_2O in surface waters

The surface (3−5 m water depth) concentrations of N_2O in the Prydz Bay (during the 31st CHINARE) were

generally low, ranging from 13.3 nmol/L to 16.1 nmol/L (mean ± std: 14.7 nmol/L ± 0.7 nmol/L). Spatially, the lowest N_2O concentrations were found in front of the Amery Ice Shelf (14.0 nmol/L ± 0.5 nmol/L), whereas the highest values were observed at about 67°–66°S (Fig. 3), where these values coincided with relatively low temperatures and salinities (Table 1). Most waters at the time of sampling were either near atmospheric equilibrium or slightly undersaturated (83%–102%; mean ± std: 94% ± 4%) (Table 1). Surface N_2O undersaturation in the Prydz Bay has been reported to be associated with physical environment variabilities, such as the input of ice-melt water and high solubility due to low temperatures (Zhan and Chen, 2009; Zhan et al., 2015). Compared with cruises, we found that the N_2O concentration was slightly higher in 2011 than in 2015 and 2006. However, the classical onshore-offshore gradient observed in most oceanic regions (Yang et al., 2020) was not attained, and no discernible temporal trend in N_2O concentrations for the period 2006−2015 could be distinguished (Fig. 3).

3.3 *Cross-shelf variability in N_2O in the Prydz Bay*

The section along 73°E from 64°S to 68°S from the 31st CHINARE was taken as a representative profile section, which covers the continental shelf and slopes to the adjacent deep ocean. The vertical profiles of N_2O were characteristically different in the Prydz Bay between the continental shelf and offshore deep ocean (Fig. 4a), which was consistent with the findings of a previous study (Zhan et al., 2015).

In the central Amery depression, the N_2O concentrations below the surface water were relatively homogeneous, ranging from 14.3 nmol/L to 17.5 nmol/L (mean ± SD: 16.5 nmol/L ± 0.5 nmol/L) throughout the water column (Fig. 4a). In contrast, N_2O distributions north of the ASF (i.e., in open ocean waters north of 67°S) clearly varied with increasing water depth (Fig. 4a). Between the ASF and about 65°S, N_2O concentrations below the surface water slowly increased and then reached a weak N_2O maximum value (about 18.8 nmol/L) between 100 m to

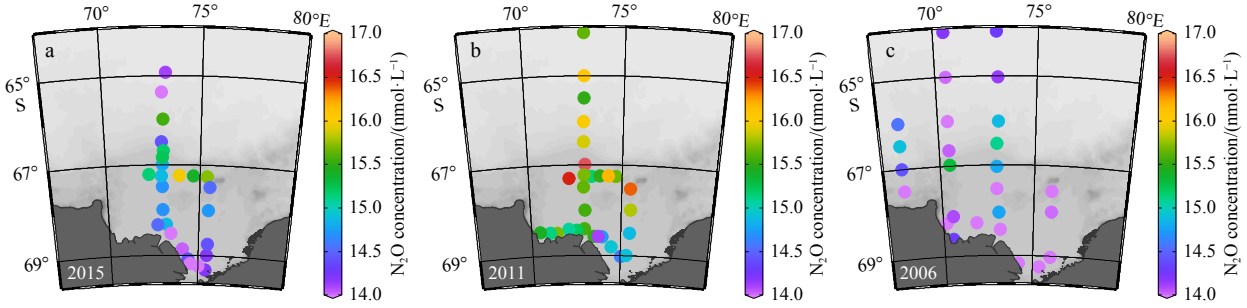


Fig. 3. Surface distributions of N_2O concentration during the 31st CHINARE (a), 27th CHINARE (b), and 22nd CHINARE (c) periods.

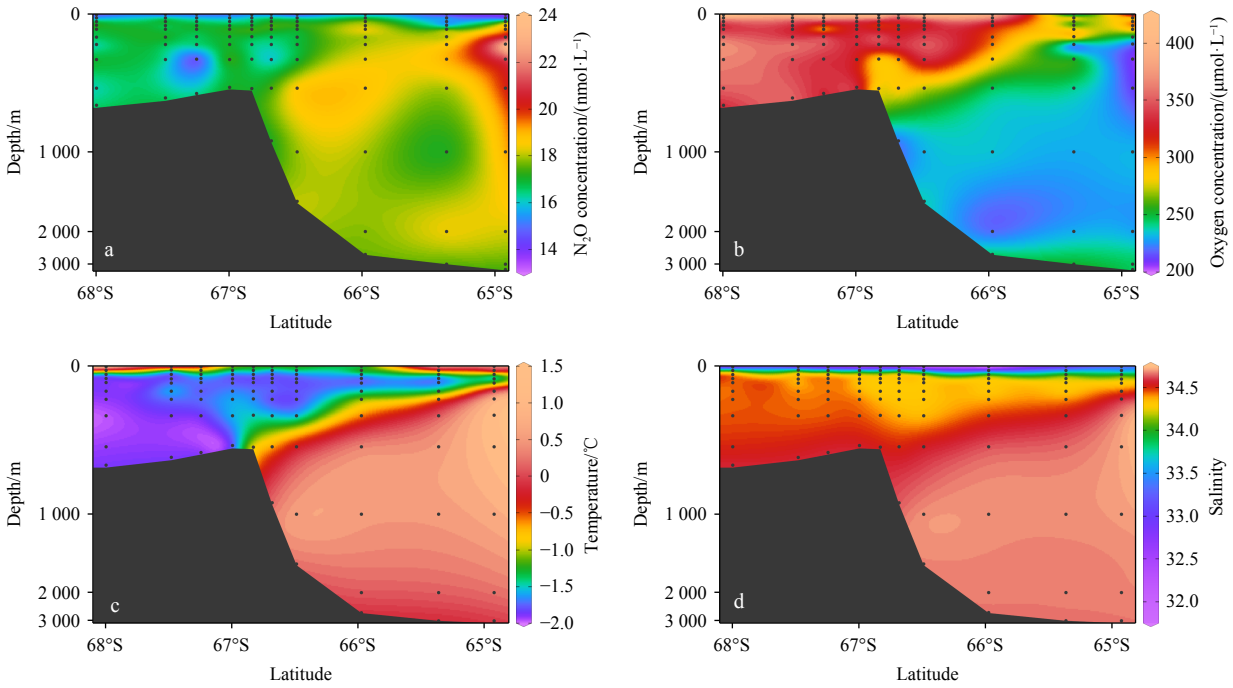


Fig. 4. Vertical profiles of N_2O concentration (a), oxygen concentration (b), temperature (c), and salinity (d) along 73°E (Section P5) during the 31st CHINARE.

500 m. However, at the northernmost station P05-1 (65°S), a steep N_2O concentration gradient and N_2O maximum (up to 23.4 nmol/L) were observed at a depth of about 200 m below the N_2O maximum layer, and N_2O concentrations gradually decreased to about 18.2 nmol/L at about 2 000 m. Below 2 000 m, N_2O concentrations were relatively constant, with a mean concentration of about 17.5 nmol/L.

4 Discussion

4.1 *Driving factors of N_2O in surface waters*

The variability of N_2O in surface waters reflects the balance between biological production/consumption and physically driven changes in solubility and/or water mass sources. Surface N_2O production by biological processes is thought to be strongly limited by light (Horrigan et al., 1981) and dissolved oxygen inhibition (Averill and Tiedje, 1982). However, recent studies have demonstrated that significant rates of nitrification can be measured in the euphotic zone (Yool et al., 2007; Beman et al., 2012), suggesting that N_2O production in the surface layer might be nonnegligible (Zamora and Oschlies, 2014). However, N_2O production through nitrification generally requires low O_2 concentrations (about 4–10 μmol/L), high ammonium (NH_4^+) (Zamora and Oschlies, 2014; Mdutyana et al., 2020) and abundant *amoA* genes (marker genes for nitrification by archaea) in surface water. In our study, the high O_2 concentrations (mean ± std: 376 μmol/L ± 42 μmol/L) measured seem to indicate inadequate conditions for nitrifiers. This is in line with the observation that rates of nitrification are generally extremely low in southern regions of the SO (Mdutyana et al., 2020, 2022). Moreover, *amoA* genes have been found to be essentially absent in the surface water of the SO (Kalanetra et al., 2009). Thus, the contribution of surface N_2O by nitrification in the Prydz Bay seems negligible.

To explore the role of physical processes as controlling factors of N_2O distribution in the Prydz Bay, we carried out multiple regression analyses of N_2O concentration vs. temperature and salinity (Fig. 5). R^2 indicates how well the regression line approximates the real data points. Our regression analysis revealed that N_2O was significantly negatively correlated with temperature during all three cruises (Pearson, $p < 0.005$), indicating that temperature affected mainly the changes in N_2O concentrations in surface waters. However, the effect of salinity on surface water is also important because the level of salinity is determined by the volume of meltwater in the sea ice region, which directly decreases the N_2O concentration in surface water (Randall et al., 2012).

We used a simple box model to calculate the N_2O mass balance in the SML [Eq. (8)]. The results revealed that the cross-pycnocline fluxes from the subsurface to the SML (F_{deep}) (mean ± std: 0.04 m/s ± 0.03 m/s in 2015, Table 2) were almost zero, indicating that the upward transport of N_2O from subsurface water was of minor importance; this results from strong stratification of the upper water column, reducing mixing between the surface

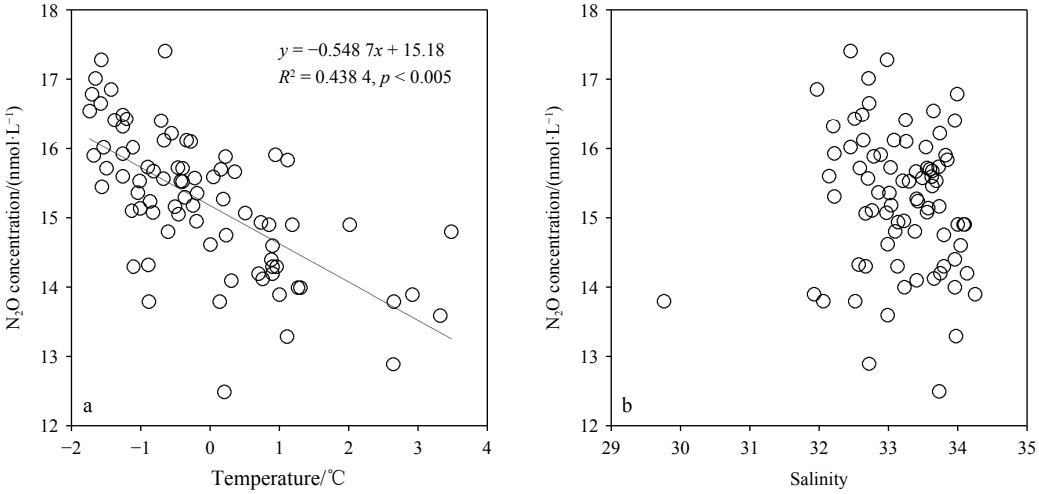


Fig. 5. Multiple regression analysis of N_2O vs. temperature (a) and salinity (b) during all three cruises.

Table 2. N_2O flux calculation in the Prydz Bay during the 31st and 27th CHINARE

Cruise	Region	N_2O flux/[μmol·(m²·d)⁻¹]		
		$F_{sea\text{-}air}$	F_{deep}	F_x
31st CHINARE	the front of Amery Ice Shelf	–2.0 ± 1.1	0.02 ± 0.03	–1.7 ± 0.9
	cross shelf	–0.2 ± 0.6	0.04 ± 0.03	–0.3 ± 0.6
27th CHINARE	the front of Amery Ice Shelf	–2.2 ± 0.8	0.04 ± 0.03	–2.3 ± 0.8
	cross shelf	–0.6 ± 0.8	0.02 ± 0.04	–0.7 ± 0.9

and N_2O-enriched subsurface waters. In this study, we had no data to calculate the contribution of integrated N_2O production in the SML; however, we assumed that the value of P_i is close to zero because N_2O production in the SML could be minor, as discussed above. In terms of the N_2O mass balance, $F_{sea\text{-}air}$ was affected mainly by melt water. $F_{sea\text{-}air}$ was mostly negative [range: –3.2 μmol/(m^2·d) to 1.4 μmol/(m^2·d); mean ± SD: –0.6 μmol/(m^2·d) ± 1.0 μmol/(m^2·d)] during the austral summer of 2015. Spatially, the lowest sea-air flux densities were observed in front of the Amery Ice Shelf. Similarly, F_x was clearly lower in front of the Amery Ice Shelf (mean ± std: –2.0 m/s ± 1.1 m/s in 2015) than in the northern region (mean ± std: –0.2 m/s ± 0.6 m/s in 2015), suggesting a greater input of meltwater, which caused dilution of N_2O in front of the Amery Ice Shelf (Randall et al., 2012; Zhan et al., 2015). These results were in line with the values of the 27th CHINARE. Thus, overall, Prydz Bay represented a weak sink of atmospheric N_2O at the time of sampling (austral summers in 2006 and 2015). During the summer, sea ice melting plays an important role in the N_2O cycle in the surface water of Prydz Bay as strong stratification, caused by sea ice melting water, hinders the vertical exchange between the subsurface and surface waters, which combined with low nitrification rates results in low N_2O production in surface waters.

4.2 *Driving factors of N_2O in subsurface waters*

The different distributions of N_2O in the Prydz Bay indicated that it was influenced by different driving factors. In general, three processes influence N_2O concentrations in the subsurface and deep layers of the ocean: *in situ* production, consumption and physical transport. The prevailing high O_2 concentrations (158−424 μmol/L) in the Prydz Bay exclude N_2O production or consumption via denitrification but favor nitrification as the main production process of N_2O in subsurface/deep waters.

The ASF and depression separate Prydz Bay into two relatively independent regions, the continental shelf and offshore deep ocean (Vaz and Lennon, 1996), with only limited exchange between them (Smith et al., 1984). Therefore, the effect of the exchange of N_2O between the continental shelf and offshore deep ocean can be considered negligible. We assumed that vertical convection and *in situ* production were possibly responsible for the observed N_2O concentration and distribution pattern on the continental shelf of Prydz Bay.

The continental shelf is a relatively high net primary productivity region (Wang et al., 2021). Considering that the shelf water column environment was well ventilated dissolved oxygen (338 μmol/L ± 29 μmol/L) (Fig. 4a), a denitrification source seems unlikely. This is further supported by the positive N^* values (understood here as deviations in the ratio of dissolved nitrogen to phosphorus from Redfield stoichiometry, i.e., $N^* = [NO_3^-] + [NO_2^-] + [NH_4^+] - 16 \times [PO_4^{3-}] + 2.9$) (Deutsch et al., 2001) and found throughout the study area (mean ± std: 2.5 μmol/L ± 4.8 μmol/L), indicating that canonical denitrification was unlikely. Linear regression between $\Delta[N_2O]$ and AOU did not reveal the expected relationship for a system where nitrification is dominant (Fig. 6a), which may result from strong vertical convection caused by increased density through the cooling of air temperature and salt rejection during sea ice formation in fall and winter, which can reach a very deep depth throughout the bay (Smith et al., 1984). We assume that the biological production of N_2O was low because low temperature inhibits enzyme activity (Sabba et al., 2015) and had a low rate of nitrification (Mdutyana et al., 2020, 2022).

Unlike those in most coastal regions, the N_2O concentrations and $\Delta[N_2O]$ values in the offshore deep ocean were higher than those in the continental shelf of Prydz Bay. A positive relationship between AOU and N_2O was observed in the offshore deep ocean (Fig. 6a). However, the profiles of N_2O clearly differed between 65°–67°S and north of 65°S. The N_2O profiles north of 65°S showed clear maxima between 150 m and 200 m, which coincided with the dissolved oxygen minimum (Fig. 4b), indicating that they were associated with the core of the upper Circumpolar Deep Water (UCDW). A similar pattern was not observed between 65° and 67°S, where the N_2O concentration was relatively low and presented N_2O subsur-

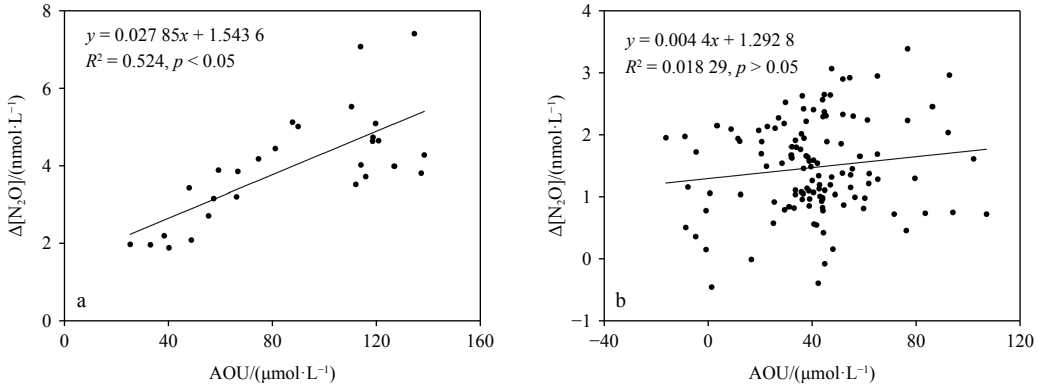


Fig. 6. Relationship between $\Delta[N_2O]$ and AOU in subsurface waters of Prydz Bay during the 31st CHINARE. a. Open ocean and b. continental shelf.

face maxima at about 150–300 m and then a very small decrease until 2 000 m. These profiles agree with those of a previous study published by Zhan et al. (2015). We assumed that hydrographic processes are likely to result in these two types of profiles. Between 65°S and 67°S, subsurface water was primarily occupied by lower Circumpolar Deep Water (LCDW) (200–2 000 m), which originated from North Atlantic Deep Water. In contrast, the water masses north of 65°S were occupied by UCDW (100–300 m) and LCDW (300–2 000 m). UCDW originates primarily from the eastern South Pacific Ocean and western Indian Ocean.

We assumed that N_2O in the eastern South Pacific Ocean/western Indian Ocean and North Atlantic Deep Water was taken into the UCDW and LCDW, respectively, and that an accumulation of N_2O occurred during transport over time (Bange and Andreae, 1999). N_2O at the starting point of the South Pacific Ocean/western Indian Ocean tends to be higher than that in North Atlantic Deep Water (Bange and Andreae, 1999), resulting in higher N_2O concentrations in the UCDW than in the LCDW. A positive linear correlation between $\Delta[N_2O]$ and AOU was observed in the offshore deep ocean (Fig. 6a), indicating that the observed N_2O accumulation over time was caused mainly by nitrification. There were no discernible differences in N_2O concentrations between 27th CHINARE (2011) and 31st CHINARE (2016) in the offshore deep ocean because the subsurface water in the SO is influenced mainly by large-scale water masses in the global circulation system, and differences cannot be observed in such a short time. However, under the influence of global climate warming and increasing sea water melting, the global circulation system might still have an important impact on the physical control of N_2O cycling in the SO.

5 Conclusions

The dissolved N_2O concentrations in the surface waters of Prydz Bay were generally low and featured undersaturated with the overlying atmosphere, such that this area was a weak sink of atmospheric N_2O at the time of sampling. A comparison with N_2O concentrations from the same region during different cruises revealed that N_2O concentrations and saturations in the surface waters were variable, but no temporal trend for the period 2006−2015 could be identified. Temperature and salinity changes played a dominant role in setting the N_2O concentrations for surface ocean waters in the Prydz Bay. Excess N_2O was observed in the offshore deep ocean below the surface layer, mostly due to N_2O accumulation from nitrification during transportation. No signs of significant N_2O production were detected in the shelf waters between 2011 and 2015.

Unlike most coastal regions, our results suggest a different pattern of N_2O distribution in the Prydz Bay (low N_2O on the continental shelf vs. high N_2O in offshore deep waters), a finding that might serve future model studies assessing N_2O emissions from the SO. To detect the interannual variability and long-term trends in dissolved N_2O concentrations in the Prydz Bay (which are in turn induced by ongoing environmental changes in the SO, such as warming and increasing atmospheric N_2O mole fractions), we suggest establishing time series measurements regularly as part of the proposed global N_2O ocean observation network.

Acknowledgements

We thank Herman W. Bange for the comments that improved this manuscript. We would like to thank the officers, captain, and crew of the R/V *Xuelong* for their help with the sampling. We also thank the scientists onboard during the cruise for providing technical assistance. We thank the physical oceanography group during the 31st CHINARE for providing the salinity and temperature data.

References

Anilkumar N, Luis A J, Somayajulu Y K, et al. 2006. Fronts, water masses and heat content variability in the Western Indian sector of the Southern Ocean during austral summer 2004. Journal of Marine Systems, 63(1–2): 20–34, doi: 10.1016/j.jmarsys.2006.04.009

Averill B A, Tiedje J M. 1982. The chemical mechanism of microbioal denitrification. FEBS Letters, 138(1): 8–12, doi: 10.1016/0014-5793(82)80383-9

Bange H W, Andreae M O. 1999. Nitrous oxide in the deep waters of the world's oceans. Global Biogeochemical Cycles, 13(4): 1127–1135, doi: 10.1029/1999GB900082

Beman J M, Popp B N, Alford S E. 2012. Quantification of ammonia oxidation rates and ammonia-oxidizing archaea and bacteria at high resolution in the Gulf of California and eastern tropical North Pacific Ocean. Limnology and Oceanography, 57(3): 711–726, doi: 10.4319/lo.2012.57.3.0711

Canadell J G, Monteiro P M S, Costa M H, et al. 2021. Global carbon and other biogeochemical cycles and feedbacks. In: Masson-Delmotte V, Zhai P, Pirani A, et al, eds. Climate Change 2021: The Physical Science Basis. Contribution of Working Group Ⅰ to the Sixth Assessment Report of the Intergovernmental Panel on Climate Change. Cambridge: Cambridge University Press, 673–816

Castellani G, Veyssière G, Karcher M, et al. 2022. Shine a light: under-ice light and its ecological implications in a changing Arctic Ocean. Ambio, 51(2): 307–317, doi: 10.1007/s13280-021-01662-3

Charpentier J, Farías L, Pizarro O. 2010. Nitrous oxide fluxes in the central and eastern South Pacific. Global Biogeochemical Cycles, 24(3): GB3011, doi: 10.1029/2008GB003388

de Boyer Montégut C, Madec G, Fischer A S, et al. 2004. Mixed layer depth over the global ocean: an examination

of profile data and a profile-based climatology. Journal of Geophysical Research: Oceans, 109(C12): C12003, doi: 10.1029/2004JC002378

Deutsch C, Gruber N, Key R M, et al. 2001. Denitrification and N_2 fixation in the Pacific Ocean. Global Biogeochemical Cycles, 15(2): 483–506, doi: 10.1029/2000GB001291

Dutton G S, Hall B D. 2023. Global atmospheric nitrous oxide hemispheric and global mean dry air mole fractions from the NOAA GML halocarbons *in situ* network, 1998–2023, Version: 2023-04-13, doi:org/10.7289/V5X0659V

Farías L, Florez-Leiva L, Besoain V, et al. 2015. Dissolved greenhouse gases (nitrous oxide and methane) associated with the naturally iron-fertilized Kerguelen region (KEOPS 2 cruise) in the Southern Ocean. Biogeosciences, 12(6): 1925–1940, doi: 10.5194/bg-12-1925-2015

Goreau T J, Kaplan W A, Wofsy S C, et al. 1980. Production of NO_2^- and N_2O by nitrifying bacteria at reduced concentrations of oxygen. Applied and Environmental Microbiology, 40(3): 526–532, doi: 10.1128/aem.40.3.526-532.1980

Grefe I, Fielding S, Heywood K J, et al. 2018. Nitrous oxide variability at sub-kilometre resolution in the Atlantic sector of the Southern Ocean. PeerJ, 6: e5100, doi: 10.7717/peerj.5100

Henley S F, Cozzi S, Fripiat F, et al. 2023. Macronutrient biogeochemistry in Antarctic land-fast sea ice: insights from a circumpolar data compilation. Marine Chemistry, 257: 104324, doi: 10.1016/j.marchem.2023.104324

Horrigan S G, Carlucci A F, Williams P M. 1981. Light inhibition of nitrification in sea-surface films. Journal of Marine Research, 39(3): 557–565

Kalanetra K M, Bano N, Hollibaugh J T. 2009. Ammonia-oxidizing *Archaea* in the Arctic Ocean and Antarctic coastal waters. Environmental Microbiology, 11(9): 2434–2445, doi: 10.1111/j.1462-2920.2009.01974.x

Koch C W, Brown T A, Amiraux R, et al. 2023. Year-round utilization of sea ice-associated carbon in Arctic ecosystems. Nature Communications, 14(1): 1964, doi: 10.1038/s41467-023-37612-8

Kurtz N T, Markus T. 2012. Satellite observations of Antarctic sea ice thickness and volume. Journal of Geophysical Research: Oceans, 117: C08025, doi: 10.1029/2012JC008141

Lin Lina, Chen Hongxia, Liu Na. 2016. The characteristics of warm water inflowing and its temporal and spatial variation on the Prydz Bay continental shelf, Antarctic. Acta Oceanologica Sinica, 35(9): 51–57, doi: 10.1007/s13131-016-0934-6

Löscher C R, Kock A, Könneke M, et al. 2012. Production of oceanic nitrous oxide by ammonia-oxidizing archaea. Biogeosciences, 9(7): 2419–2429

Mashayek A, Ferrari R, Merrifield S, et al. 2017. Topographic enhancement of vertical turbulent mixing in the Southern Ocean. Nature Communications, 8(1): 14197

Mdutyana M, Sun Xin, Burger J M, et al. 2022. The kinetics of ammonium uptake and oxidation across the Southern Ocean. Limnology and Oceanography, 67(4): 973–991

Mdutyana M, Thomalla S J, Philibert R, et al. 2020. The seasonal cycle of nitrogen uptake and nitrification in the Atlantic sector of the Southern Ocean. Global Biogeochemical Cycles, 34(7): e2019GB006363, doi: 10.1029/2019GB006363

Middleton J H, Humphries S E. 1989. Thermohaline structure and mixing in the region of Prydz Bay, Antarctica. Deep-Sea Research Part A. Oceanographic Research Papers, 36(8): 1255–1266

Nevison C D, Keeling R F, Weiss R F, et al. 2005. Southern Ocean ventilation inferred from seasonal cycles of atmospheric N_2O and O_2/N_2 at Cape Grim, Tasmania. Tellus B: Chemical and Physical Meteorology, 57(3): 218–229

Randall K, Scarratt M, Levasseur M, et al. 2012. First measurements of nitrous oxide in Arctic sea ice. Journal of Geophysical Research: Oceans, 117(C9): C00G15

Ravishankara A R, Daniel J S, Portmann R W. 2009. Nitrous oxide (N_2O): the dominant ozone-depleting substance emitted in the 21st century. Science, 326(5949): 123–125

Rees A P, Bange H W, Arévalo-Martínez D L, et al. 2022. Nitrous oxide and methane in a changing Arctic Ocean. Ambio, 51(2): 398–410

Rees A P, Owens N J P, Upstill-Goddard R C. 1997. Nitrous oxide in the Bellingshausen sea and drake passage. Journal of Geophysical Research: Oceans, 102(C2): 3383–3391

Resplandy L, Hogikyan A, Müller J D, et al. 2024. A synthesis of global coastal ocean greenhouse gas fluxes. Global Biogeochemical Cycles, 38(1): e2023GB007803, doi: 10.1029/2023GB007803

Sabba F, Picioreanu C, Pérez J, et al. 2015. Hydroxylamine diffusion can enhance N_2O emissions in nitrifying biofilms: a modeling study. Environmental Science & Technology, 49(3): 1486–1494

Sabu P, Subeesh M P, Sivakrishnan K K, et al. 2021. Causes and impacts of anomalous warming in the Prydz Bay, East Antarctica during austral summer 2016–17. Polar Science, 30: 100660, doi: 10.1016/j.polar.2021.100660

Sallee J B 2018. Southern Ocean warming. Oceanography, 31(2): 52–62

Shadwick E H, Tilbrook B, Williams G D. 2014. Carbonate chemistry in the Mertz Polynya (East Antarctica): biological and physical modification of dense water outflows and the export of anthropogenic CO_2. Journal of Geophysical Research: Oceans, 119(1): 1–14, doi: 10.1002/2013JC009286

Smith N R, Zhaoqian D, Kerry K R, et al. 1984. Water masses and circulation in the region of Prydz Bay, Antarctica. Deep-Sea Research Part A. Oceanographic Research Papers, 31(9): 1121–1147

St-Laurent P, Yager P L, Sherrell R M, et al. 2017. Pathways and supply of dissolved iron in the Amundsen Sea (Antarctica). Journal of Geophysical Research: Oceans, 122(9): 7135–7162

Sun Weiping, Hu Chuanyu, Han Zhengbing, et al. 2012. Distribution of nutrients and Chl *a* in Prydz Bay during the aus-

tral summer of 2011. Chinese Journal of Polar Research (in Chinese), 24(2): 178–186, doi: 10.3724/SP.J.1084.2012.00178

Thomas D N, Kattner G, Engbrodt R, et al. 2001. Dissolved organic matter in Antarctic sea ice. Annals of Glaciology, 33: 297–303, doi: 10.3189/172756401781818338

Thomson A J, Giannopoulos G, Pretty J, et al. 2012. Biological sources and sinks of nitrous oxide and strategies to mitigate emissions. Philosophical Transactions of the Royal Society B: Biological Sciences, 367(1593): 1157–1168

Tian Hanqin, Xu Rongting, Canadell J G, et al. 2020. A comprehensive quantification of global nitrous oxide sources and sinks. Nature, 586(7828): 248–256, doi: 10.1038/s41586-020-2780-0

Toyoda S, Yoshida O, Yamagishi H, et al. 2019. Identifying the origin of nitrous oxide dissolved in deep ocean by concentration and isotopocule analyses. Scientific Reports, 9(1): 7790, doi: 10.1038/s41598-019-44224-0

Vaz R A N, Lennon G W. 1996. Physical oceanography of the Prydz Bay region of Antarctic waters. Deep-Sea Research Ⅰ: Oceanographic Research Papers, 43(5): 603–641, doi: 10.1016/0967-0637(96)00028-3

Wang Yanmin, Qi Di, Wu Yingxu, et al. 2021. Biological and physical controls of pCO_2 and air-sea CO_2 fluxes in the austral summer of 2015 in Prydz Bay, East Antarctica. Marine Chemistry, 228: 103897, doi: 10.1016/j.marchem.2020.103897

Wanninkhof R. 2014. Relationship between wind speed and gas exchange over the ocean revisited. Limnology and Oceanography: Methods, 12(6): 351–362, doi: 10.4319/lom.2014.12.351

Weiss R F. 1970. The solubility of nitrogen, oxygen and argon in water and seawater. Deep-Sea Research and Oceanographic Abstracts, 17(4): 721–735, doi: 10.1016/0011-7471(70)90037-9

Weiss R F, Price B A. 1980. Nitrous oxide solubility in water and seawater. Marine Chemistry, 8(4): 347–359, doi: 10.1016/0304-4203(80)90024-9

Weiss R F, Van Woy F A, Salameh P K, et al. 1992. Surface Water and Atmospheric Carbon Dioxide and Nitrous Oxide Observations by Shipboard Automated Gas Chromatography: Results from Expeditions between 1977 and 1990. Oak Ridge: Oak Ridge National Lab., 1–123

Williams G D, Aoki S, Jacobs S S, et al. 2010. Antarctic bottom water from the Adélie and George V land coast, East Antarctica (140°–149°E). Journal of Geophysical Research: Oceans, 115(C4): C04027

Wong A P S, Bindoff N L, Forbes A. 1985. Ocean-ice shelf interaction and possible bottom water formation in Prydz Bay, Antarctica. In: Jacobs S S, Weiss R F, eds. Ocean, Ice, and Atmosphere: Interactions at the Antarctic Continental Margin. Washington: American Geophysical Union, 173–187

Yang S, Chang B X, Warner M J, et al. 2020. Global reconstruction reduces the uncertainty of oceanic nitrous oxide emissions and reveals a vigorous seasonal cycle. Proceedings of the National Academy of Sciences of the United States of America, 117(22): 11954–11960

Ye Wangwang, Arévalo-Martínez D L, Li Yuhong, et al. 2023. Significant methane undersaturation during austral summer in the Ross Sea (Southern Ocean). Limnology and Oceanography Letters, 8(2): 305–312, doi: 10.1002/lol2.10315

Yool A, Martin A P, Fernández C, et al. 2007. The significance of nitrification for oceanic new production. Nature, 447(7147): 999–1002, doi: 10.1038/nature05885

Zamora L M, Oschlies A. 2014. Surface nitrification: a major uncertainty in marine N_2O emissions. Geophysical Research Letters, 41(12): 4247–4253, doi: 10.1002/2014GL060556

Zhan Liyang, Chen Liqi. 2009. Distributions of N_2O and its air-sea fluxes in seawater along cruise tracks between 30°S-67°S and in Prydz Bay, Antarctica. Journal of Geophysi−cal Research: Oceans, 114(C3): C03019, doi: 10.1029/2007JC004406

Zhan Liyang, Chen Liqi, Zhang Jiexia, et al. 2013. A system for the automated static headspace analysis of dissolved N_2O in seawater. International Journal of Environmental Analytical Chemistry, 93(8): 828–842, doi: 10.1080/03067319.2012.702273

Zhan Liyang, Chen Liqi, Zhang Jiexia, et al. 2015. Austral summer N_2O sink and source characteristics and their impact factors in Prydz Bay, Antarctica. Journal of Geophysical Research: Oceans, 120(8): 5836–5849, doi: 10.1002/2015JC010944

Zhang Xinning, Ward B B, Sigman D M. 2020. Global nitrogen cycle: critical enzymes, organisms, and processes for nitrogen budgets and dynamics. Chemical Reviews, 120(12): 5308–5351, doi: 10.1021/acs.chemrev.9b00613